Journal of King Saud University – Science (2015) 27, 338–348

King Saud University
Journal of King Saud University – Science
www.ksu.edu.sa
www.sciencedirect.com

ORIGINAL ARTICLE

Unsteady MHD free convective Couette flow between vertical porous plates with thermal radiation

Basant K. Jha [a], **B.Y. Isah** [b,*], **I.J. Uwanta** [b]

[a] *Department of Mathematics, Ahmadu Bello University, Zaria, Nigeria*
[b] *Department of Mathematics, Usmanu Danfodiyo University, Sokoto, Nigeria*

Received 11 July 2014; accepted 21 June 2015
Available online 2 July 2015

KEYWORDS

MHD;
Couette flow;
Thermal radiation;
Free-convective flow;
Implicit finite difference

Abstract This study investigates the unsteady MHD free convective Couette flow of viscous incompressible electrically conducting fluid between two infinite vertical porous plates in the presence of transverse magnetic field and thermal radiation. Solutions for time dependent energy and momentum equations are obtained by the implicit finite difference method. To check the accuracy of the numerical solutions, steady state solutions for energy and momentum equations are obtained by using the perturbation method. The effect of various parameters controlling the physical situation is discussed with the aid of line graphs. Significant results from this study are that both velocity and temperature increase with the increase in thermal radiation parameter and time. A series of numerical experiments show that steady state velocity and temperature occur when the dimensionless time approaches the values of Prandtl number of the fluid. During the course of numerical computation, an excellent agreement was found between unsteady and steady state solutions at large value of time.

1. Introduction

The literature on steady and unsteady free convective flow phenomenon in vertical plates associated with Couette flow with or without porosity or MHD is numerous. Many studies have been conducted on steady state Couette flow under different physical situations (Tsangaris et al., 2007; Barletta and Magyari, 2008; Chen and Zhu, 2008; Chaughan and Rastogi, 2012) while many others considered their investigation on unsteady Couette flow problems (Dash and Biswal, 1989; Zhu and De Kee, 2007; Raptis, 2011; Salama, 2011; Seth et al., 2012; Jha et al., 2013).

MHD free convective Couette flow has been studied with kin interest due to its possible applications in many industrial problems. For example, in the power industry, among the methods of generating electric power is one in which electrical energy is extracted directly from a moving conducting fluid Ibrahim et al. (2008). Chaughan and Rastogi (2012) studied

* Corresponding author.
E-mail addresses: basant777@yahoo.co.uk (B.K. Jha), isahby1973@gmail.com (B.Y. Isah), imeuwanta@yahoo.com (I.J. Uwanta).
Peer review under responsibility of King Saud University.

ELSEVIER Production and hosting by Elsevier

http://dx.doi.org/10.1016/j.jksus.2015.06.005
1018-3647

steady state MHD Couette flow of a viscous, incompressible and electrically conducting fluid flow between two infinite parallel plates in the presence of an inclined magnetic field. Hayat et al. (2004) considered Hydromagnetic Couette flow of an Oldroyd-B fluid in a rotating system of a viscous, incompressible and electrically conducting fluid bounded between two rigid non-conducting parallel plates. Moreover, several authors have studied excellent works on unsteady MHD free-convective flow between vertical parallel porous plates. Hazem (2010a,b) reported unsteady magnetohydromagnetic Couette flow of an electrically conducting incompressible non-Newtonian viscoelastic fluid between two parallel horizontal non-conducting porous plates with heat transfer. Salama (2011) investigated flow formation in Couette motion in magnetohydrodynamics with time varying suction and taking into account the effects of heat and mass transfer. Khem (2012) analyzed MHD Couette motion of an electrically conducting, viscous incompressible fluid through saturated porous medium bounded by two insulated vertical porous plates. Farhad et al. (2012) investigated the hydromagnetic rotating flow of viscous fluid through a porous space under slip condition. Baoku et al. (2012) studied the problem of steady hydromagnetics Couette flow of a high viscous fluid through a porous channel in the presence of an applied uniform transverse magnetic field and thermal radiation.

The present work is motivated to study Unsteady MHD free-convective Couette flow between vertical porous plates with thermal radiation.

2. Mathematical analysis

Consider a time dependent unsteady free convective Couette flow of a viscous, incompressible, electrically conducting and radiating fluid between two infinite vertical parallel porous plates in the presence of transverse magnetic field as shown in Fig. 1. At time, $t' \leqslant 0$ both the fluid and porous plates are assumed to be at rest at temperature T_0. At some time, $t' > 0$ the temperature of the porous plate situated at $y' = 0$ rises to T_w and starts moving in its own plane with impulsive motion with velocity U while the other porous plate at a distance H from it is fixed and maintained at temperature T_0. A uniform magnetic field of strength B_0 is imposed normal to the porous plates. The Cartesian (x', y') co-ordinate systems are taken with x'-axis along the moving porous plate in the vertical upward direction and the y'-axis normal to it. Since the porous plates are of infinite length, the velocity and temperature are functions of y' and t' alone. Using Boussinesq's approximation, the governing equations for the present physical situation in dimensional form are:

$$\frac{\partial u'}{\partial t'} + V_0 \frac{\partial u'}{\partial y'} = \nu \frac{\partial^2 u'}{\partial y'} + g\beta(T' - T_0) - \frac{\sigma_1 B_0^2 u'}{\rho} \tag{1}$$

$$\frac{\partial T'}{\partial t'} + V_0 \frac{\partial T'}{\partial y'} = \alpha \left[\frac{\partial^2 T'}{\partial y'^2} - \frac{1}{K} \frac{\partial q_r}{\partial y'} \right] \tag{2}$$

where T_0 is the initial temperature of the fluid and porous plates, T' is the dimensional temperature of the fluid, α is the thermal diffusivity, K is the thermal conductivity, ρ is the density of the fluid, β is the coefficient of the thermal expansion, σ_1 is the fluid electrical conductivity and B_0 is the strength of applied magnetic field. The flow is assumed laminar and fully developed.

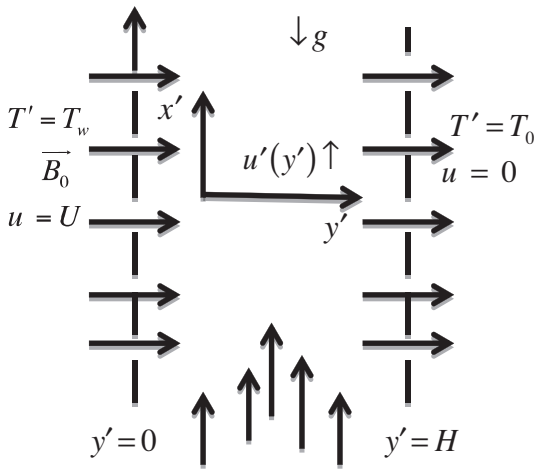

Figure 1 Schematic diagram of the problem.

The quantity q_r appearing on the right hand side of Eq. (2) represents the radiative heat flux in the y'-direction where the radiative heat flux in the x'-direction is considered insignificant in comparison with that in the y'-direction. The radiative heat flux term in the problem is simplified by using the Rosseland diffusion approximation for an optically thick fluid according to (Hossaini et al., 1999; Aydin and Kaya, 2009; Rashad, 2009; Ali Agha et al., 2014).

$$q_r = -\frac{4\sigma \partial T'^4}{3\kappa^* \partial y'} \tag{3}$$

where σ is Stefan–Boltzmann constant and k^* is the mean absorption coefficient. This approximation is valid for intensive absorption, that is, for an optically thick boundary layer. Despite these shortcomings, the Rosseland approximation has been used with success in a variety of problems ranging from the transport of radiation through gases at low density to the study of the effects of radiation on blast waves by nuclear explosion Ali et al. (Ali Agha et al., 2014).

The required initial and boundary conditions to be satisfied are

$$\begin{aligned} &t' \leqslant 0 : u' = 0,\ T' = T_0,\ 0 \leqslant y' \leqslant H \\ &t' \geqslant 0 : \begin{cases} u' = U,\ T' = T_w, \text{ at } y' = 0 \\ u' = 0,\ T' = T_0, \text{ at } y' = H \end{cases} \end{aligned} \tag{4}$$

The dimensionless quantities used in the present problem are

$$\begin{aligned} &t = t'v/H,\ y = y'/H,\ u = u'/U \\ &Pr = v/\alpha,\ M^2 = \sigma_1 B_0^2 H^2/\rho v \\ &Gr = g\beta H^2 (T_w - T_0)/Uv \\ &R = 4\sigma (T' - T_0)^3/\kappa^* K,\ C_T = T_0/(T_w - T_0) \\ &\theta = (T' - T_0)/(T_w - T_0),\ S = V_0 H/v \end{aligned} \tag{5}$$

By introducing the dimensionless quantities defined in Eq. (5), Eqs. (1) and (2) in dimensionless form are

$$\frac{\partial u}{\partial t}+S\frac{\partial u}{\partial y}=\frac{\partial^2 u}{\partial y^2}+Gr\theta-M^2u \tag{6}$$

$$Pr\left[\frac{\partial\theta}{\partial t}+S\frac{\partial\theta}{\partial y}\right]=\left[1+\frac{4R}{3}(C_T+\theta)^3\right]\frac{\partial^2\theta}{\partial y^2}+4R[C_T+\theta]^2\left(\frac{\partial\theta}{\partial y}\right)^2 \tag{7}$$

subject to the dimensionless initial and boundary conditions

$$\begin{aligned} &t\leqslant 0: u=0,\ \theta=0,\ 0\leqslant y\leqslant 1\\ &t\geqslant 0: \begin{cases} u=1,\ \theta=1,\ \text{at } y=0\\ u=0,\ \theta=0,\ \text{at } y=1\end{cases}\end{aligned} \tag{8}$$

3. Analytical solution

The governing equations presented in the previous section are highly nonlinear and exhibited no analytical solutions. In general such solution can be very useful in validating computer routines of complicated time dependent two or three-dimensional free convective and radiating conducting fluid and comparison with experimental data. It is therefore of interest to reduce the governing equations of the present problem to the form that can be solved analytically. A special case of the present problem that exhibits analytical solution is the problem of steady state MHD free-convective Couette flow between vertical porous plates with thermal radiation. The resulting steady state equations and boundary conditions for this special case can be written as

$$0=\frac{d^2u}{dy^2}-S\frac{du}{dy}-M^2u+Gr\theta \tag{9}$$

$$0=\left[1+\frac{4R}{3}(C_T+\theta)^3\right]\frac{d^2\theta}{dy^2}+4R[C_T+\theta]^2\left(\frac{d\theta}{dy}\right)^2-SPr\frac{d\theta}{dy} \tag{10}$$

the boundary conditions are

$$\begin{aligned} &u=1\ \theta=1 \text{ at } y=0\\ &u=0\ \theta=0 \text{ at } y=1\end{aligned} \tag{11}$$

To construct analytical solutions of Eqs. (9) and (10) subject to (11), it is assumed that the radiation parameter is small and taking a power series expansion in the radiation parameter R employs a regular perturbation method.

$$\left.\begin{aligned}\theta(y)&=\theta_0(y)+R\theta_1(y)+0(R)\\ u(y)&=u_0(y)+Ru_1(y)+0(R)\end{aligned}\right\} \tag{12}$$

Substituting Eq. (12) into Eqs. (9) and (10) and equating the coefficient of like powers of, R the required solutions of the governing steady state momentum and energy equations are

$$\begin{aligned}u(y)=&Ae^{(x_1y)}+Be^{(-x_2y)}+D_0+D_1e^{(SPry)}\\&+R[A_1e^{(x_1y)}+B_1e^{(-x_2y)}+D_2+(D_4+D_8)e^{(SPry)}\\&+D_5e^{(4SPry)}+D_6e^{(2SPry)}+D_7e^{(3SPry)}]\end{aligned} \tag{13}$$

$$\begin{aligned}\theta(y)=&\frac{e^{(SPry)}-e^{(SPr)}}{1-e^{(SPr)}}+\left[\frac{-C_3}{SPr}+C_4e^{(SPry)}\right.\\&\left.+\frac{yF_1e^{(SPry)}}{SPr}+\frac{F_2e^{(4SPry)}}{4[SPr]^2}+\frac{F_3e^{(2SPry)}}{2[SPr]^2}+\frac{F_4e^{(3SPry)}}{6[SPr]^2}\right]\end{aligned} \tag{14}$$

From (13) the steady-state skin frictions on the boundaries are:

$$\begin{aligned}u'(y)|_{y=0}=&x_1A-x_2B+SPrD_1+[x_1A_1-x_2B_1\\&-D_3+SPr(D_4+D_8)+4D_5SPr\\&+2D_6SPr+3D_7SPr]\end{aligned} \tag{15}$$

$$\begin{aligned}u'(1)|_{y=1}=&x_1Ae^{(x_1)}-x_2e^{(-x_2)}+S\mathrm{Pr}D_1Ae^{(SPr)}\\&+R\left[x_1A_1e^{(x_1)}-x_2B_1e^{(-x_2)}+D_3e^{(SPr)}\right.\\&+SPr(D_3+D_4+D_8)e^{(SPr)}\\&+4SPrD_5e^{(4SPr)}+2SPrD_6e^{(2SPr)}\\&\left.+3SPrD_7e^{(3SPr)}\right]\end{aligned} \tag{16}$$

Also from (14) the steady-state Nusselt numbers on the boundaries are:

$$\begin{aligned}\theta'(0)|_{=0}=&\tfrac{SPr}{1-e^{(SPr)}}+R\left[SPrC_4+\tfrac{F_1}{[SPr]}\right.\\&\left.+\tfrac{F_2}{3[SPr]}+\tfrac{F_3}{[SPr]}+\tfrac{F_4}{2[SPr]}\right]\end{aligned} \tag{17}$$

$$\begin{aligned}\theta'(1)|_{=1}=&\frac{SPre^{(SPr)}}{1-e^{(SPr)}}+R\left[SPrC_4+F_1e^{(SPr)}\right.\\&\left.+\frac{F_1e^{(SPr)}}{[SPr]}+\frac{F_2e^{(4SPr)}}{3[SPr]}+\frac{F_3e^{(3SPr)}}{[SPr]}+\frac{F_4e^{(3SPr)}}{2[SPr]}\right]\end{aligned} \tag{18}$$

4. Numerical solution procedure

The nonlinear momentum and energy equations given in (6) and (7) are solved under the appropriate initial and boundary condition (8) by the implicit finite difference method. The transport Eqs. (6), (7) at the grid point (i, j) are expressed in difference form using Taylor's expansion. The momentum equation reads.

$$\frac{u_i^{j+1}-u_i^j}{\Delta t}+S\frac{u_{i+1}^j-u_i^j}{\Delta y}=\frac{u_{i-1}^{j+1}-2u_i^{j+1}+u_{i+1}^{j+1}}{(\Delta y)^2}-M^2u_i^j+\theta_i^j \tag{19}$$

and the energy equation becomes

$$\begin{aligned}Pr\frac{\theta_i^{j+1}-\theta_i^j}{\Delta t}+SPr\frac{\theta_{i+1}^j-\theta_i^j}{\Delta y}=&[1+\frac{4R}{3}(C_T+\theta)^3]\\&\times\left(\frac{\theta_{i-1}^{j+1}-2\theta_i^{j+1}+\theta_{i+1}^{j+1}}{(\Delta y)^2}\right)+4R\left[C_T+\theta_i^j\right]^2\left(\frac{\theta_{i+1}^j-\theta_{i-1}^j}{(2\Delta y)}\right)^2\end{aligned} \tag{20}$$

with the following initial and boundary conditions:

$$\left.\begin{aligned}&u_{i,0}=0,\quad \theta_{i,0}=0 \text{ for all } i=0\\&u_{0,j}=1,\quad \theta_{0,j}=1\\&u_{M,j}=0,\quad \theta_{M,j}=0\end{aligned}\right\} \tag{21}$$

Thus the values of u and θ at grid point $t = 0$ are known; hence the temperature field has been solved at time $t_{i+1}=t_i+\Delta t$ using the known values of the previous time $t = t_i$ for all $i=1,2,\rightleftharpoons,N-1$. Then the velocity field is

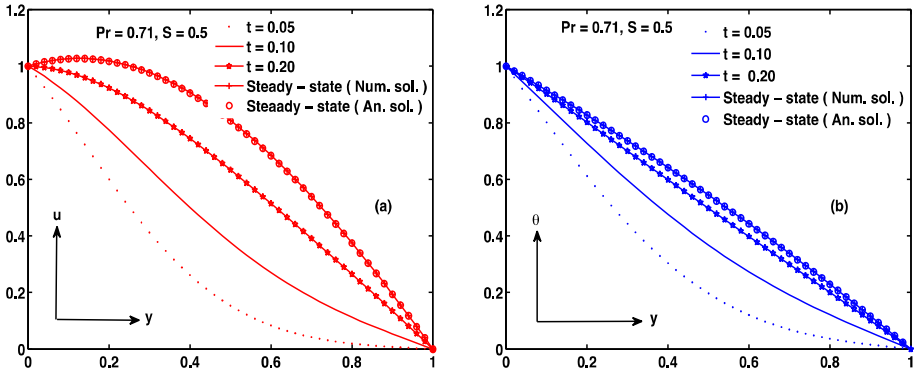

Figure 2 Velocity profile ($R = 0.0001,\ C_T = 0.01,\ M = 1,\ Gr = 5$).

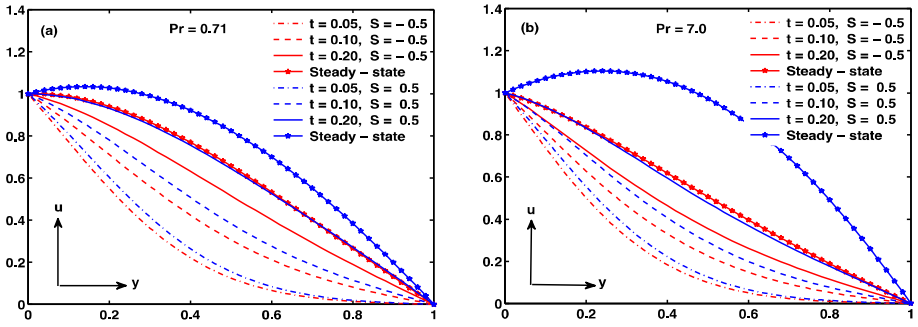

Figure 3 Velocity profile ($R = 0.2,\ C_T = 0.1,\ M = 1,\ Gr = 5$).

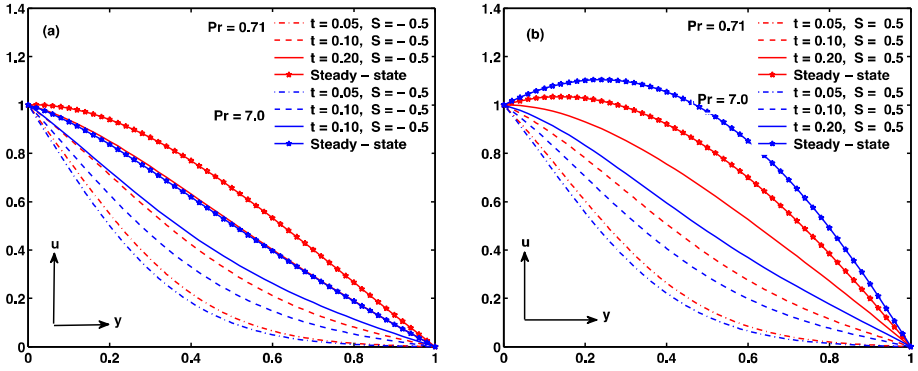

Figure 4 Velocity profile ($R = 0.2,\ C_T = 0.1,\ M = 1,\ Gr = 5$).

evaluated using the already known value of temperature field obtained at $t_{i+1} = t_i + \Delta t$. These processes are repeated till the required solution of u and θ is gained at convergence criteria.

$$abs|(u,\theta)_{exact} - (u,\theta)num| < 10^{-3} \tag{22}$$

The analytical solutions derived in Section 3 are used to check the accuracy and effectiveness of the numerical procedure. For large values of time a steady state condition is reached which corresponds to the steady state solution obtained analytically by using the perturbation technique. A comparison between analytical and corresponding numerical results is presented in Fig. 2.

5. Results and discussion

Numerical calculation on velocity field and temperature field using the finite difference method is performed with the help of the dimensionless parameters that govern the flow. The parameters are the magnetic parameter (M), the radiation parameter (R), the temperature difference (C_T), the Grashof number (Gr) taken greater than zero that corresponds to external cooling of the moving porous plate, suction/injection parameter (S) simultaneously opposite to porous plates at the same rate and the Prandtl number (Pr) chosen as 0.71 and 7.0 that physically represent two fluids air and water,

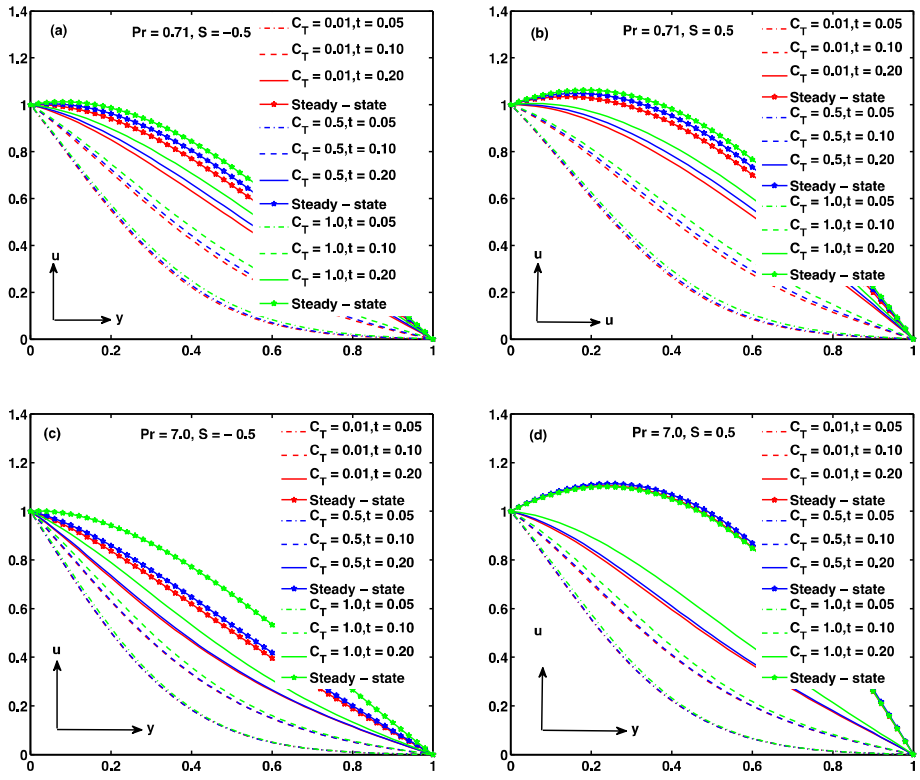

Figure 5 Velocity profile ($R = 0.2,\ M = 1,\ Gr = 5$).

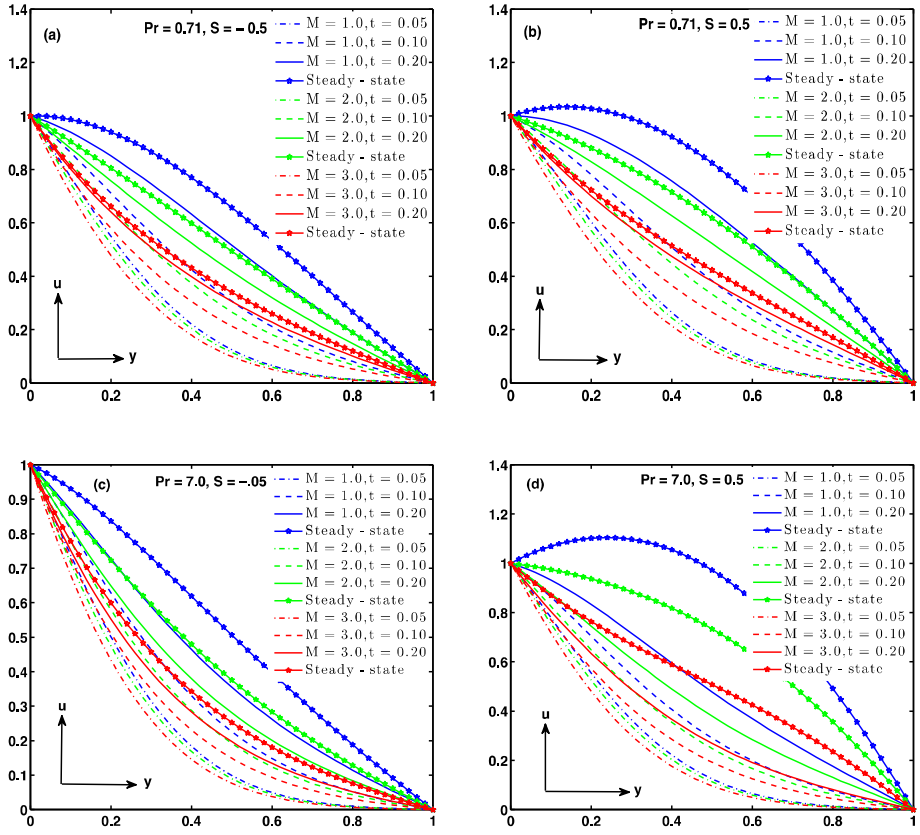

Figure 6 Velocity profile ($R = 0.2,\ Gr = 5,\ C_T = 0.1$).

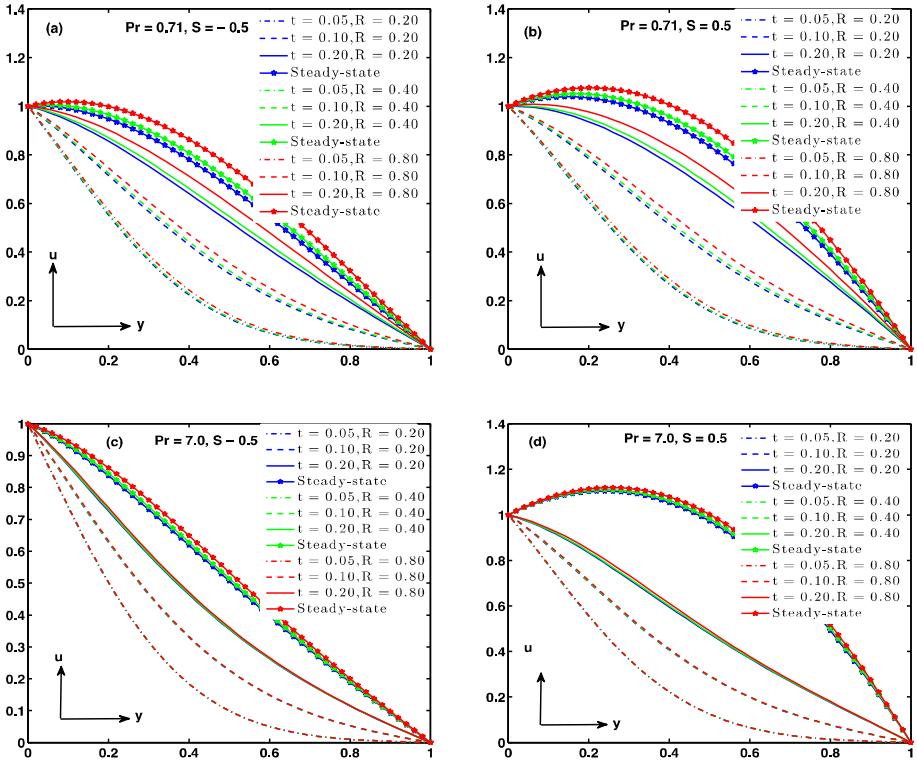

Figure 7 Velocity profile ($Gr = 5,\ M = 1,\ C_T = 0.1$).

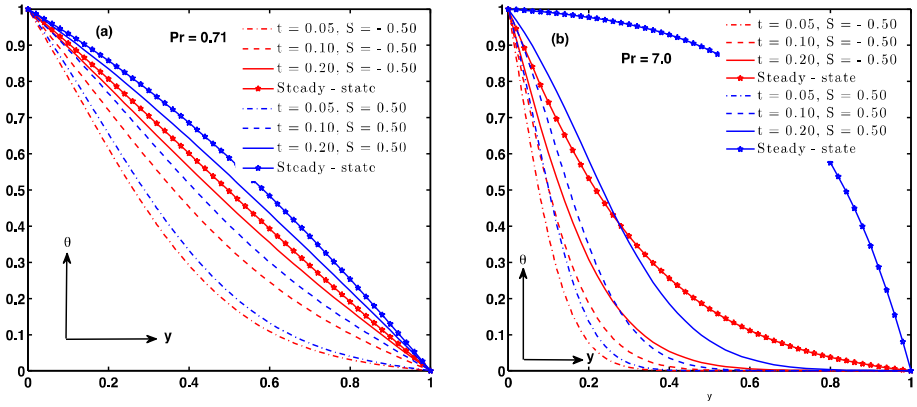

Figure 8 Temperature profile ($R = 0.2,\ C_T = 0.1$).

respectively. Moreover, time is chosen between $0.05 \leqslant t \leqslant 8.5$ so as to capture the transient behavior of both velocity and temperature. In the present numerical computation the numerical values of R are in range of $0 \leqslant R \leqslant 0.8$. A large value of, R leads to finite time temperature blow up since the terms associated with R are strong heat sources (Makinde and Chinyoka, 2010). Besides, all other parameters are taken arbitrary. To clearly report the influence of the flow governing parameters on velocity, temperature, skin friction and Nusselt number figures have been shown graphically in Fig. 2 through 24. The numerical scheme was validated using the steady state (perturbation) solution obtained from Eqs. (13) and (14); and our results are found in good agreement between numerical and perturbation solution in a steady state situation as depicted in Fig. 2. Fig. 3a and b describes the influence of S and t on velocity profile. This figure reports that as time increases the velocity (air and water) increases and attains steady state. The figure reveals that when injection ($S > 0$) takes place at, $y = 0$ the fluid velocities (air and water) are higher compared with suction ($S < 0$). Fig. 4 illustrates the effect of Prandtl number (Pr) under the influence of suction and injection respectively. It is observed that the velocity of air ($Pr = 0.71$) is higher than water ($Pr = 7.0$) for $S < 0$ as shown in Fig. 4a while fluid velocity of air ($Pr = 0.71$) is less than water ($Pr = 7.0$) for $S > 0$ as narrated in Fig. 4b. The

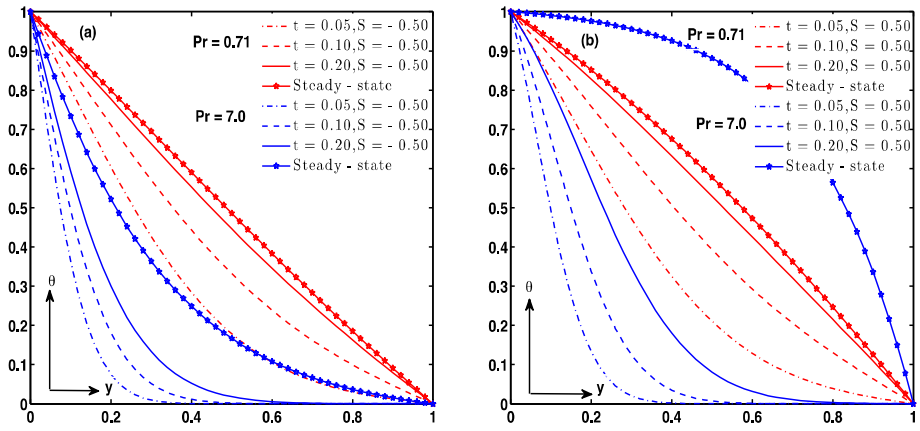

Figure 9 Temperature profile ($R = 0.2,\ C_T = 0.1$).

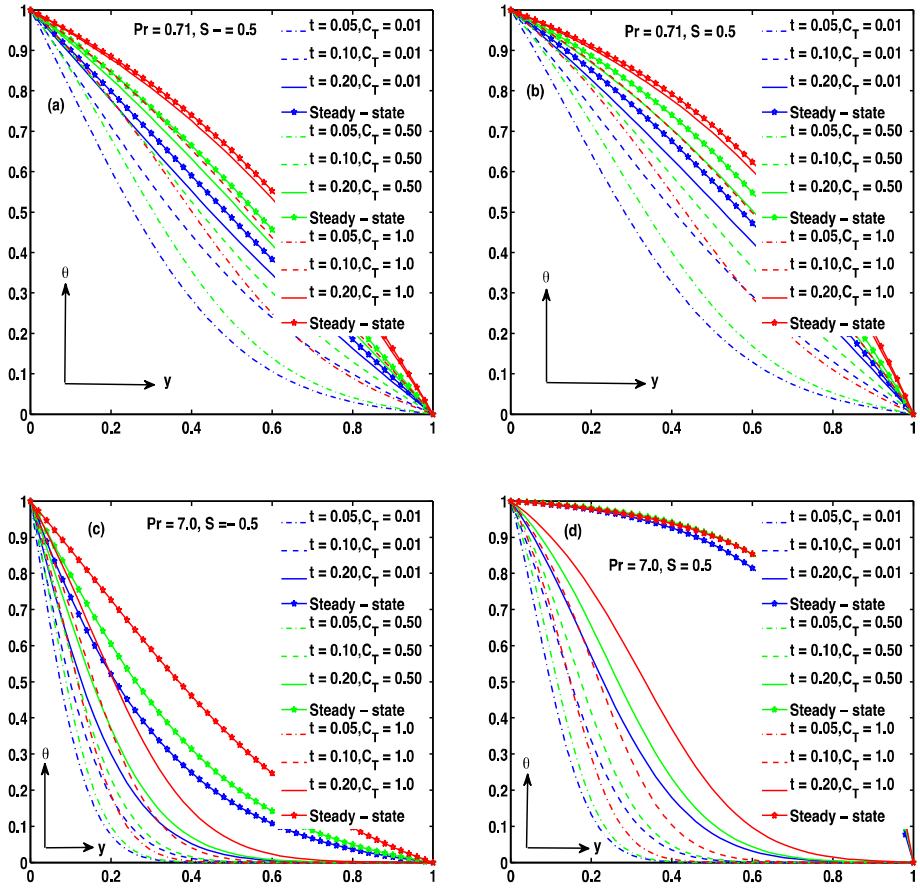

Figure 10 Temperature profile ($R = 0.2$).

inspection of the temperature difference parameter C_T is drawn in Fig. 5. The result shows that velocity increases with an increase in C_T. In Fig. 5d the role of C_T is insignificant on velocity in case of water ($Pr = 7.0$) during steady state with injection at $y = 0$ and suction at $y = 1$ which is not true when there is injection at $y = 1$ and suction at $y = 0$ as presented in Fig. 5c. However, it is interesting to mention that during steady and unsteady state, the impact of C_T is more pronounced in air than water whether suction or injection applied at $y = 0$ or $y = 1$ see Fig. 5a and b in comparison with Fig. 5c and d.

The magnetic parameter M produces resistive force, which acts in the opposite direction to the fluid motion as illustrated in Fig. 6. The impact of this can be clearly seen in Fig. 6a–d respectively, that as magnetic parameter M increases the velocity decreases for both air and water.

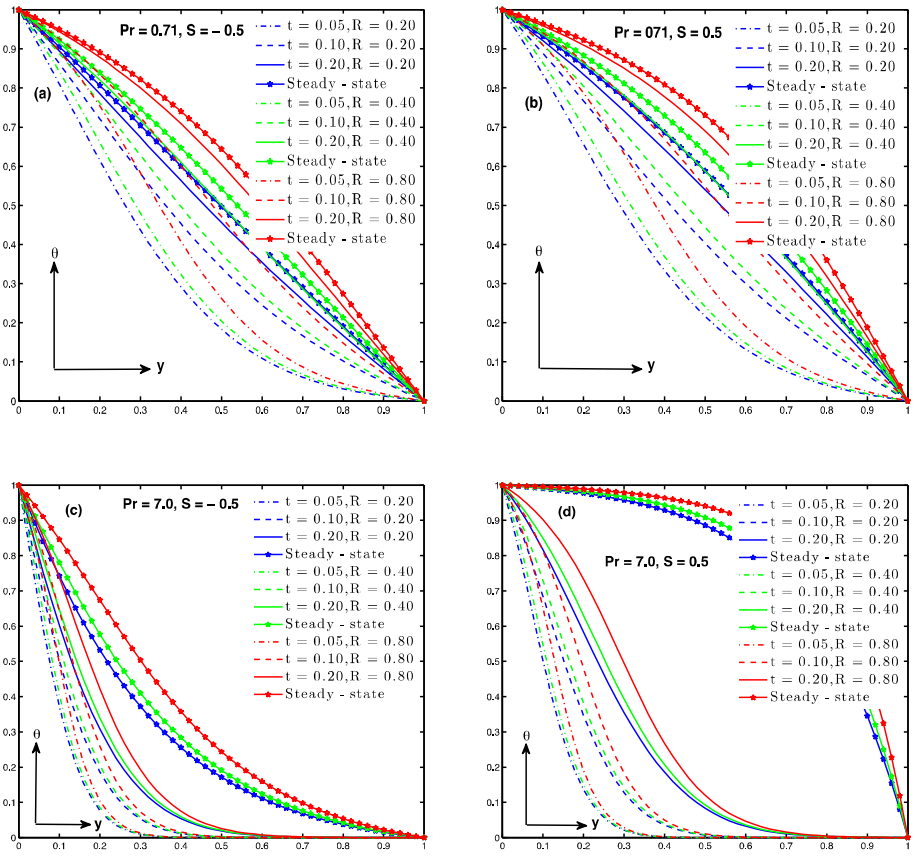

Figure 11 Temperature profile ($C_T = 0.1$).

In Fig. 7 velocity increases as radiation parameter increases. Also, it is evident from Fig. 7a–d that the impact of R is more significant incase of air than water.

The influence of S and t on temperature profile as seen in Fig. 8(a–d) tells us that as time increases the temperature (air and water) increases and attains steady state value. The figure portrays that when injection ($S > 0$) takes place at $y = 0$ the temperature (air and water) is higher compared with suction ($S < 0$) at $y = 0$.

Fig. 9 delineates the effect of Prandtl number (Pr) on temperature profile under the influence of suction and injection respectively. It is observed that the temperature of air ($Pr = 0.71$) is higher than water ($Pr = 7.0$) for $S < 0$ as depicted in Fig. 9a. It is interesting to note that at steady state the temperature is higher for water ($Pr = 7.0$) in comparison with air ($Pr = 0.71$) once injection is applied at, $y = 0$ as illustrated in Fig. 10b which is not true in case of suction. However, during unsteady state the temperature is high incase of air in comparison with water for both suction and injection see Fig. 9a and b respectively. This is due to the physical fact that, as the Prandtl number increases; the thermal diffusivity of the fluid reduces which results in a corresponding decrease in the fluid temperature.

From Fig. 10 it is noted that the temperature increases with time and temperature difference parameter (C_T) and finally attains its steady state (see Fig. 10(a–d)). Furthermore, the steady state temperature is higher in case of water ($Pr = 7.0$) when injection takes place at $y = 0$ in comparison with suction at $y = 0$ (see Fig. 10c and d).

In Fig. 11, the unsteady and steady state temperature distribution for different values of radiation parameter R and time t is outlined. It is recorded that temperature increases significantly as R increases. In addition, there is a strong influence of R on temperature variation specifically in steady situation where injection is imposed at $y = 0$ in contrast with suction at $y = 0$ in case of water ($Pr = 7.0$), as seen in Fig. 11c and d respectively.

In Figs. 12 and 13, the variation of skin friction for air ($Pr = 0.71$) and water ($Pr = 7.0$) at the plate $y = 0$ is narrated. Fig. 12 depicts the variation of skin friction with respect to C_T and time. From the set out of this figure it is voice-over that the skin friction increases with time and ultimately reaches its steady state value. It is observed from this figure that as C_T increases the skin friction increases.

Fig. 13(a–d) shows the description profiles for skin friction for different values of t and radiation parameter R. These figures reflect that, as time increases the skin friction increases until steady state is achieved. It is interesting to emphasize that the numerical value of a skin friction is higher for injection ($S > 0$) in comparison with suction ($S < 0$) acting at $y = 0$. Furthermore, the steady state skin friction values for air ($Pr = 0.71$) are larger than that of water ($Pr = 7.0$) in case of suction ($S < 0$) while it does the reverse in the case of injection ($S > 0$) acting at $y = 0$.

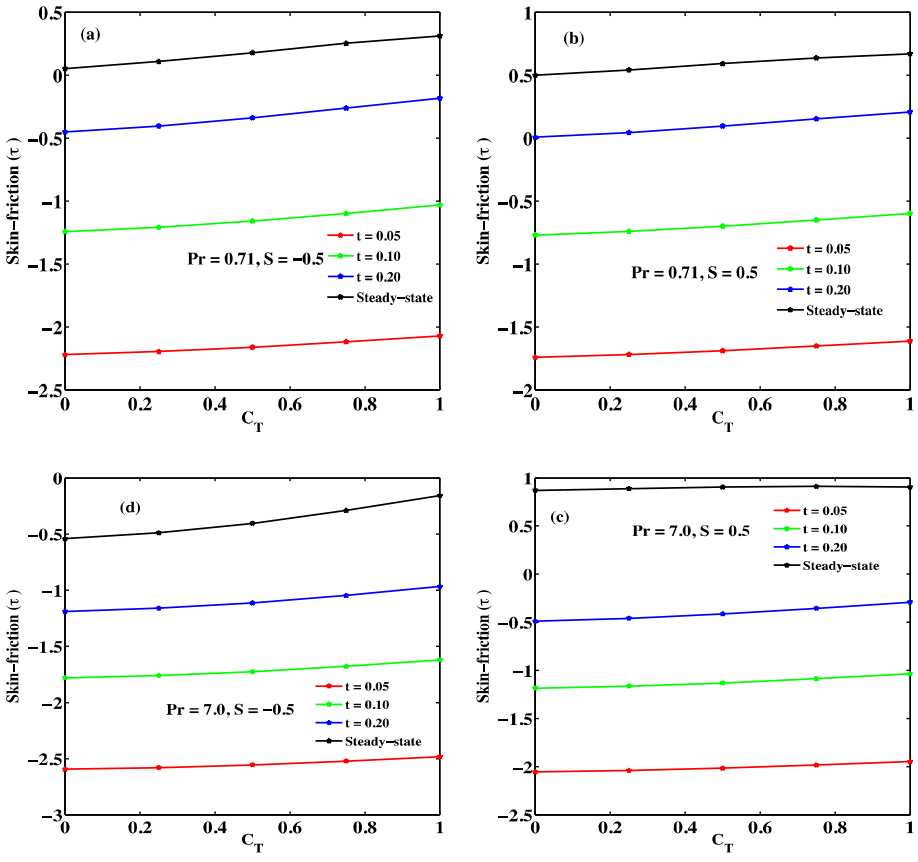

Figure 12 Skin frictions against C_T at $y = 0$.

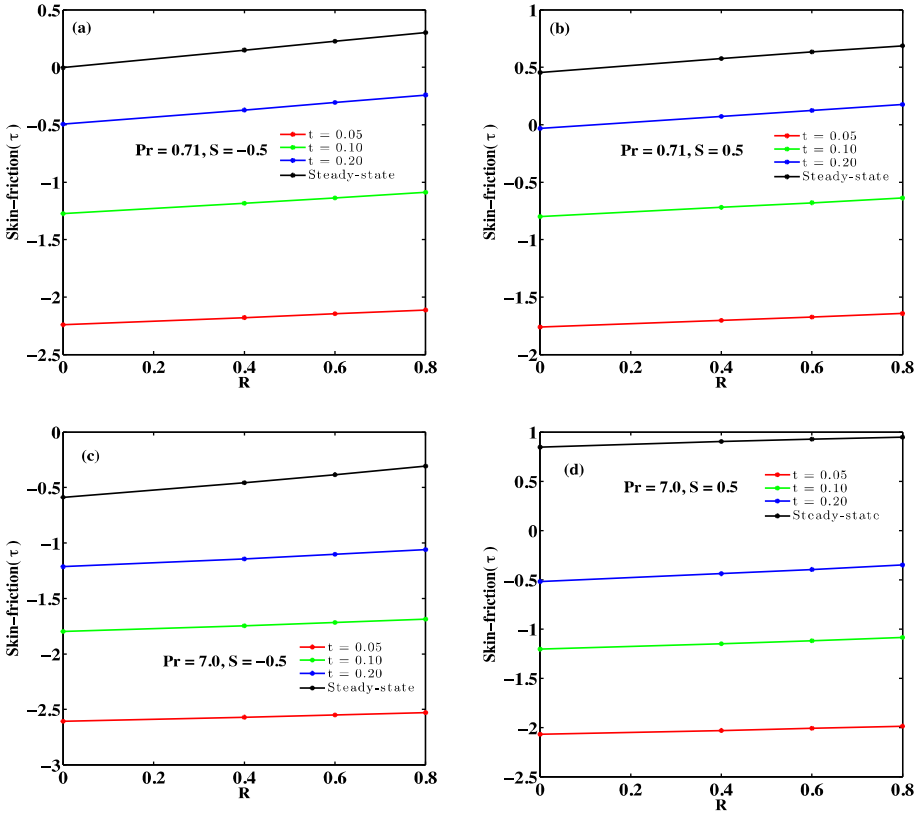

Figure 13 Skin frictions against R at $y = 0$.

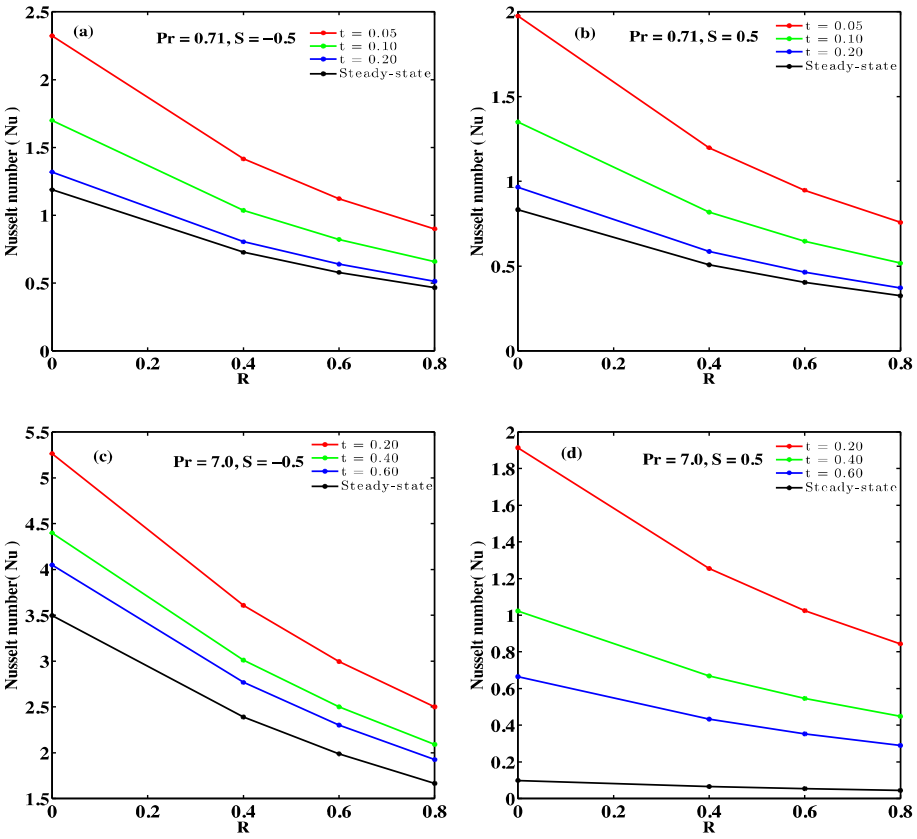

Figure 14 Nusselt numbers against R at $y = 0$.

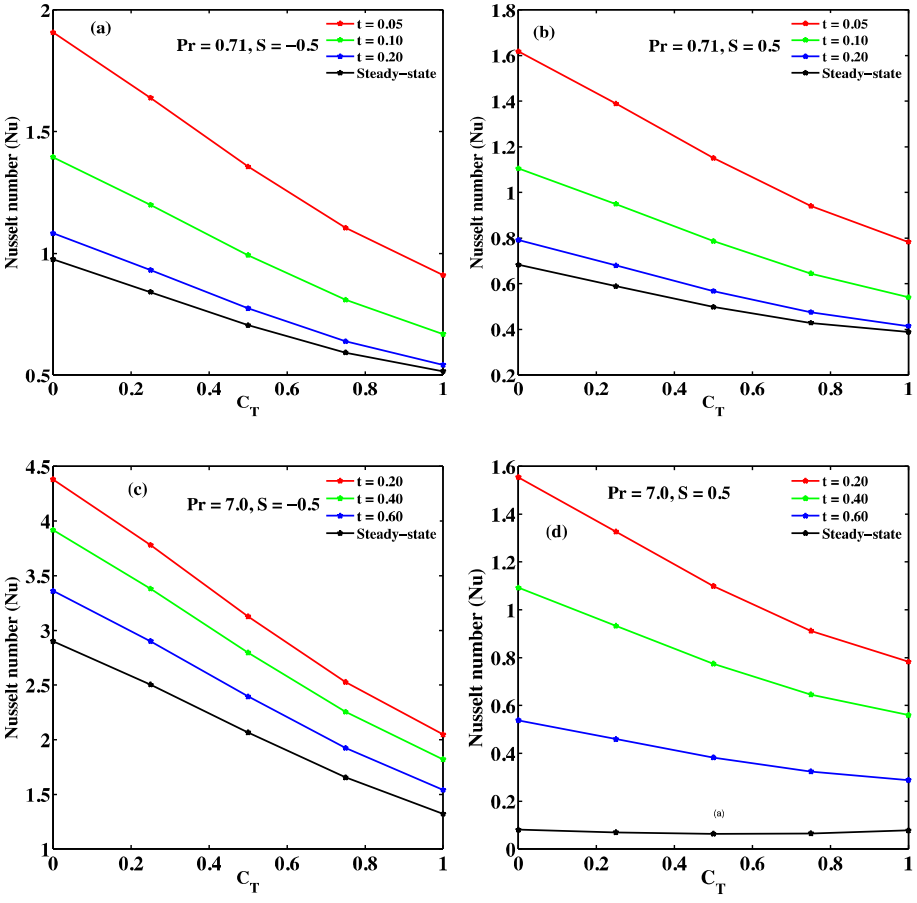

Figure 15 Nusselt numbers against C_T at $y = 0$.

Figs. 14 and 15 also sketch out the landmark influence of radiation parameter and temperature difference on Nusselt number (rate of heat transfer) at plates $y = 0$. In Fig. 14(a–d) and Fig. 15(a–d) as R or C_T increases Nusselt number decreases for considered values of, S Pr and t respectively. Furthermore, it is remarkable to point out that the impacts of R and C_T on Nusselt number are more prominent due to suction for $S < 0$ either air or water. From the figures it is also clear that the role of C_T and R is more pronounced in case of water ($Pr = 7.0$) in comparison with air ($Pr = 0.71$).

6. Conclusion

The solution of unsteady MHD free-convective Couette flow of a viscous, incompressible and electrically conducting fluid between vertical porous plates with thermal radiation is acquired. The steady state solutions for the non-linear partial differential equations are obtained by the well known perturbation series method while the implicit finite difference technique is used to solve the unsteady equations. The influence of the dimensionless parameters on velocity temperature, skin friction and Nusselt number is demonstrated on figures and discussed. From the results obtained, the findings are:

i. Velocity and temperature field increases with increase in time.
ii. Skin-friction increases with increase in time, while Nusselt number decreases with increase in time.
iii. Skin friction is always higher in the case of air ($Pr = 0.71$) in comparison with water ($Pr = 7.0$) when suction takes place at $y' = 0$, while the situation is just reverse with injection at $y' = 0$.
iv. The rate of heat transfer is higher at porous plate $y' = 0$ when suction takes place than injection.
v. Moreover, the time required for the velocity and temperature fields, skin-friction and Nusselt number to attain steady-state strongly rests on the dimensionless parameters M, R, C_T, Gr and Pr.
vi. The results are found in good agreement between steady state and unsteady solution after some sufficiently large time (t).
vii. Also during the numerical computation it is observed that time required to reach steady state is directly proportional to the nature (Prandtl number) of working fluid. Furthermore, convection current is strong as radiation parameter increases.

Acknowledgement

One of the authors Isah B. Yabo is thankful to Usmanu Danfodiyo University, Sokoto for financial support.

References

Ali Agha, H., Bouaziz, M.N., Hanini, S., 2014. Free convection boundary layer flow from a vertical flat plate embedded in a Darcy porous medium filled with a nanofluid: effects of Magnetic field and thermal radiation. Arab J. Sci. Eng. 39, 8331–8340.
Aydin, O., Kaya, A., 2009. MHD mixed convective heat transfer flow about an inclined plate. Heat Mass Transfer 46, 129–136.
Baoku, I.G., Israel-Cookey, C., Olajuwon, B.I., 2012. Magnetic field and thermal radiation effects on steady Hydromagnetic Couette flow through a porous channel. Surv. Math. Appl. 5, 215–228.
Barletta, A., Magyari, E., 2008. Buoyant Couette–Bingham flow between vertical parallel plates. Int. J. Therm. Sci. 47 (7), 811–819.
Chaughan, D., Rastogi, P., 2012. Heat transfer effects on a rotating MHD Couette flow in a channel partially by a porous medium with hall current. J. Appl. Sci. Eng. 15 (3), 281–290.
Chen, Y., Zhu, K., 2008. Couette–Poiseuille flow of Bingham fluids between two porous parallel plates with slip conditions. J. Nonnewton. Fluid Mech. 153, 1–11.
Dash, G.C., Biswal, S., 1989. Commencement of Couette flow on Oldroyd with heat sources. Indian J. Pure Appl. Math. 20 (3), 267–275.
Farhad, A., Norzieha, M., Sharidan, S., Khan, I., Samiulhaq, 2012. Hydromagnetic rotating flow in a porous medium with slip condition and Hall current. Int. J. Phys. Sci. 7 (10), 1540–1548.
Hayat, T., Nadeen, S., Asghar, S., 2004. Hydromagnetic flow of an Oldroyd-B fluid in a rotating system. Int. J. Eng. Sci. 42, 65–78.
Hazem, A.A., 2010a. Unsteady MHD Couette flow of a viscoelastic fluid with heat transfer. Kragujevac J. Sci. 32, 5–15.
Hazem, A.A., 2010b. The effect of suction and injection on unsteady Couette flow with variable properties. Kragujevac J. Sci. 32, 17–24.
Hossaini, M.A., Alim, M.A., Rees, D.A.S., 1999. The effect of radiation on free convection from a porous vertical plate. Int. J. Heat Mass Transf. 42, 181–191.
Ibrahim, F.S., Elaiw, A.M., Bakr, A.A., 2008. Effect of the chemical reaction and radiation absorption on the unsteady MHD free convection flow past a semi infinite vertical permeable moving plate with heat source and suction. Commun. Nonlinear Sci. Numer. Simul. 13, 1056–1066.
Jha, B.K., Samaila, A.K., Ajibade, A.O., 2013. Unsteady natural convection couette flow of a reactive viscous fluid in a vertical channel. Comput. Math. Model. 24 (3), 432–440.
Khem, C., Rakesh, K., Shavnam, S., 2012. Hydromagnetic oscillatory vertical Couette flow of radiating fluid through porous medium with slip and jump boundary conditions. Int. J. Phys. Math. Sci. 3 (1), 82–90.
Makinde, O.D., Chinyoka, T., 2010. Numerical investigation of transient heat transfer to hydromagnetic channel flow with radiative heat and convective cooling. Commun. Nonlinear Sci. Numer. Simul. 15, 3919–3930.
Raptis, A., 2011. Free convective oscillatory flow and mass transfer past a porous plate in the presence of radiation of an optically thin fluid. Therm. Sci. 15 (3), 849–857.
Rashad, A.M., 2009. Perturbation analysis for radiative effect on free convection flows in porous medium in the presence of pressure work and viscous dissipation. Commun. Nonlinear Sci. Numer. Simul. 14, 140–153.
Salama, F.A., 2011. Convective heat and mass transfer in a non-newtonian flow formation in a Couette motion in magnetohydrodynamics with time- varying suction. Therm. Sci. 15 (3), 749–758.
Seth, G.S., Nandkeolyar, R., Ansari, Md.S., 2012. Effects of hall current and rotation on unsteady MHD Couette flow in the presence of an inclined magnetic field. J. Appl. Fluid Mech. 5 (2), 67–74.
Tsangaris, S., Nikas, C., Tsangaris, G., Neofytou, P., 2007. Couette flow of a Bingham plastic in a channel with equally porous parallel walls. J. Nonnewton. Fluid Mech. 144, 42–48.
Zhu, H., De Kee, D., 2007. A numerical study for the cessation of Couette flow of non-Newtonian fluids with a yields stress. J. Non-Newtonian Mech. 143, 64–70.